UNDERSTANDING UNMIXED AVIRIS IMAGES IN CUPRITE, NV USING COINCIDENT HYDICE DATA

Alexander F. H. Goetz[1,2] and Bruce Kindel[1]

[1]Center for the Study of Earth from Space/CIRES,
[2]Department of Geological Sciences
University of Colorado, Boulder CO 80309

1. INTRODUCTION

For more than a decade, techniques for determining the relative abundance of materials within a pixel have been applied to multispectral and hyperspectral images from sensors such as Landsat and AVIRIS (Adams et al., 1993; Boardman, 1993). It has been difficult if not impossible to verify the correctness of the results objectively because no supporting data, such as field spectral reflectance measurements, could be acquired in sufficient quantity and at appropriate scales. In this paper we analyze data sets that, for the first time, give insight into the accuracy of unmixing analysis of AVIRIS images and also place bounds on the minimum detectable size of unique components within a pixel.

2. DATA ACQUISITION

As a part of a campaign to analyze the quality and utility of the data from the recently-completed airborne imaging spectrometer HYDICE (Hyperspectral Data and Information Collection Experiment) (Basedow et al., 1995), images were collected over Cuprite, NV on June 22, 1995. The next day, AVIRIS made an overpass of the same region. Both overpasses were made within one hour of local noon providing the highest radiance values possible at this latitude. Field spectral measurements, using an ASD Inc. FieldSpec®-FR instrument, were made of Stonewall Playa and several artificial targets laid out on the playa surface. A second set of spectral measurements of natural surfaces as well as additional targets were made on December 20, 1995. The targets were sheets of 10 mil Mylar and crushed dolomite having an average particle size of approximately 1 cm. The Mylar was laid out on the playa as was one 3x3 m target of dolomite. In the area south of Kaolinite Hill, dolomite targets ranging in size from 3.5 m to 30 cm on a side were laid out in an arc and surveyed in using differential GPS.

Figure 1 shows the area chosen for analysis as imaged by AVIRIS and HYDICE. AVIRIS is flown at an altitude of 20 km yielding a pixel size of approximately 18 m while HYDICE was flown at an altitude of 7.6 km, or 6.0 km above the surface, resulting in a 3 m pixel. Therefore, there are 36 HYDICE pixels for every AVIRIS pixel.

3. DATA REDUCTION AND ANALYSIS

Both the AVIRIS and HYDICE data sets were reduced to apparent reflectance using the empirical-line method in which field spectra of light and dark targets are used to determine gain and offset values for each of the wavelength channels. Figure 2 shows the field spectra taken on December 20 of Stonewall Playa and the area of desert pavement southwest of Kaolinite Hill used in the empirical-line calibration. An average spectrum of sagebrush clumps is also shown. These clumps cover 5-10 % of the surface of the desert pavement.

Figure 3 shows average spectra from both sensors taken from small patches in low and high reflectance areas. The coincidence of the spectra is greatest in the dark areas and poorest in the light areas. The source of these differences may be in the reduction to apparent reflectance but is not yet understood. This result points to areas of uncertainty when comparing spectra from the two different sensors.

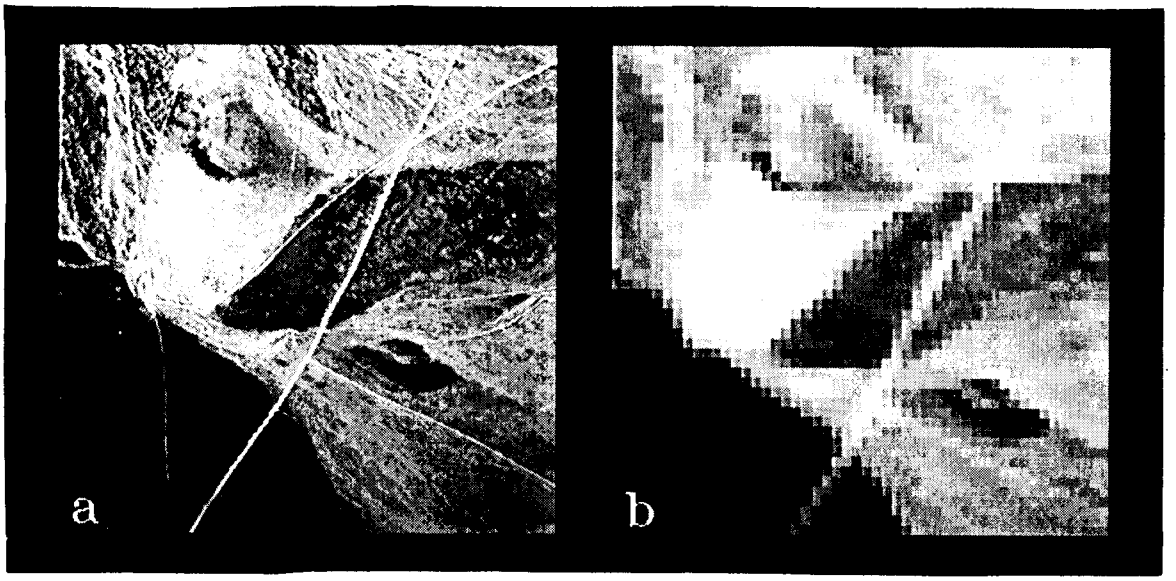

Figure 1. (a) HYDICE image at 0.8 μm of an approximately 1x1 km area south and east of Kaolinite Hill at Cuprite, NV. (b) Subset of a 20x20 km AVIRIS image of the same region as (a).

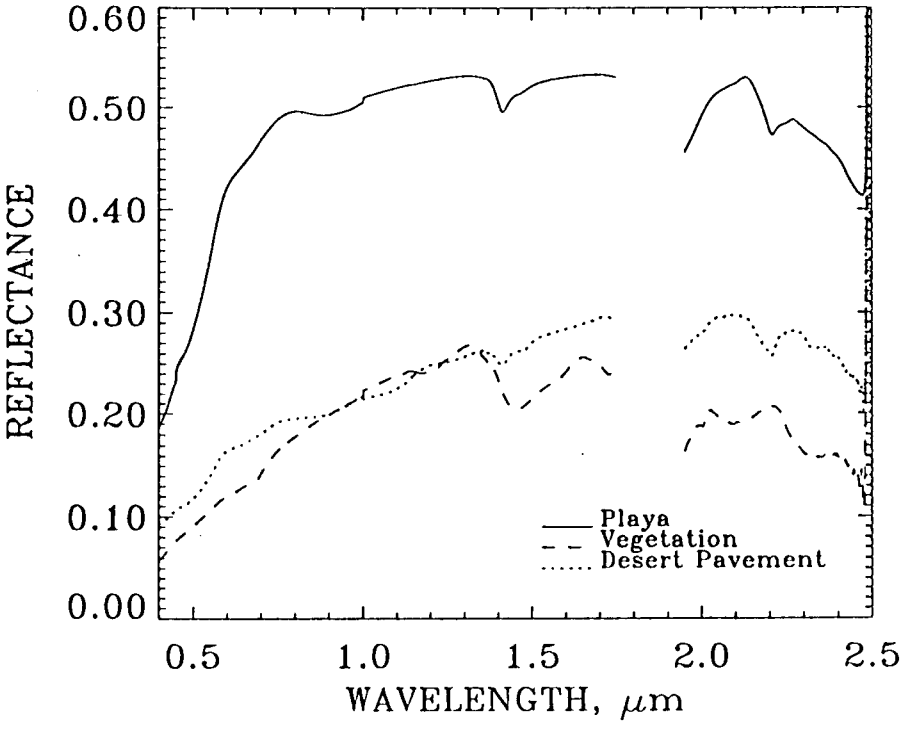

Figure 2. Field spectral measurements of Stonewall Playa and an area of desert pavement south of Kaolinite Hill used in the empirical line calibration to reduce both HYDICE and AVIRIS data to apparent reflectance.

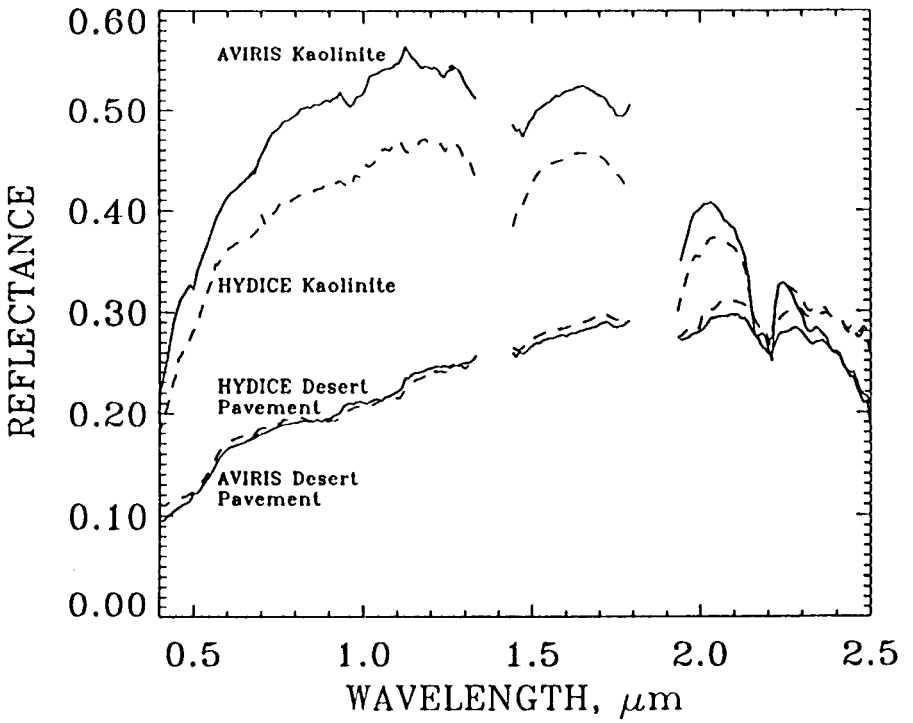

Figure 3. Comparison of AVIRIS and HYDICE pixel spectra of two regions. An average of 3 AVIRIS and 136 HYDICE pixels were used in the spectra displayed.

4. UNMIXING

The goal of unmixing analysis is to identify and quantify the component surface materials that make up individual pixels in hyperspectral images. The technique used here was unconstrained unmixing using end members derived from the HYDICE images. This algorithm is contained in the ENVI software package (Research Systems, Inc., 1995). The accurate selection of end members is one of the major uncertainties in unmixing analysis. By calibrating both datasets to the same areas in the scene, variations in atmospheric transmission and scattering as well as sensor calibration were removed. Using image-derived end members reduced an additional uncertainty associated with the relationship of the average spectrum of a heterogeneous pixel and library spectra of pure materials.

Figure 4 shows the HYDICE pixel spectra of the 5 end members chosen. The small pixel size of HYDICE made it possible to choose "pure" end members. This selection would not be possible with the coarser AVIRIS pixels. In spite of the 3 m pixels available from HYDICE, all the end member spectra are the result of mixtures of surface materials that were observed in the field to be heterogenous on a scale of one centimeter or less. Potential errors associated with this natural scale of heterogenity must be taken into account when unmixing analysis is undertaken using field or laboratory spectra as end members.

5. RESULTS

Figures 5-8 are HYDICE / AVIRIS pairs of unmixed images of the region shown in figure 1. The most striking feature is the factor of six ratio in the linear pixel dimension. The other most obvious feature common to all the figures is the overall good match between the abundances of each of the end member materials depicted as gray levels, with the lighter tones indicating higher abundances. In general the darkest tones represent negative abundances that are inevitable in an unconstrained unmixing analysis.

The kaolinite end member abundance is shown in figure 5. The major difference between the HYDICE and AVIRIS images is in the differentiation between the hilltop of relatively pure kaolinite and the colluvium draining down the eastern slope. This differentiation is obvious on the HYDICE image but not on the AVIRIS image.

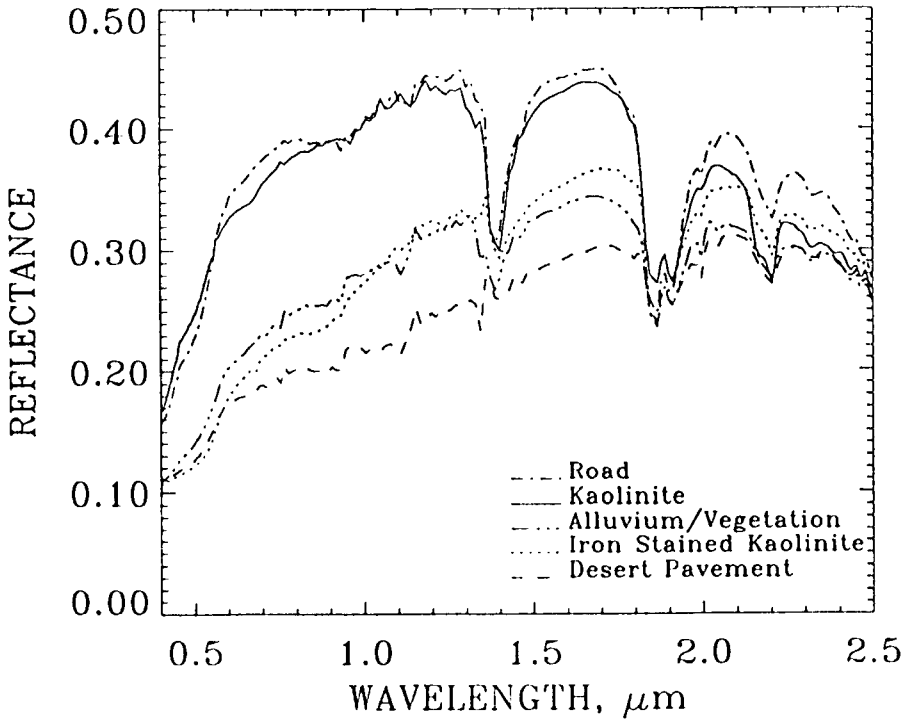

Figure 4. Reflectance spectra of end members taken from HYDICE pixels, picked visually as representative of the purest regions in each class.

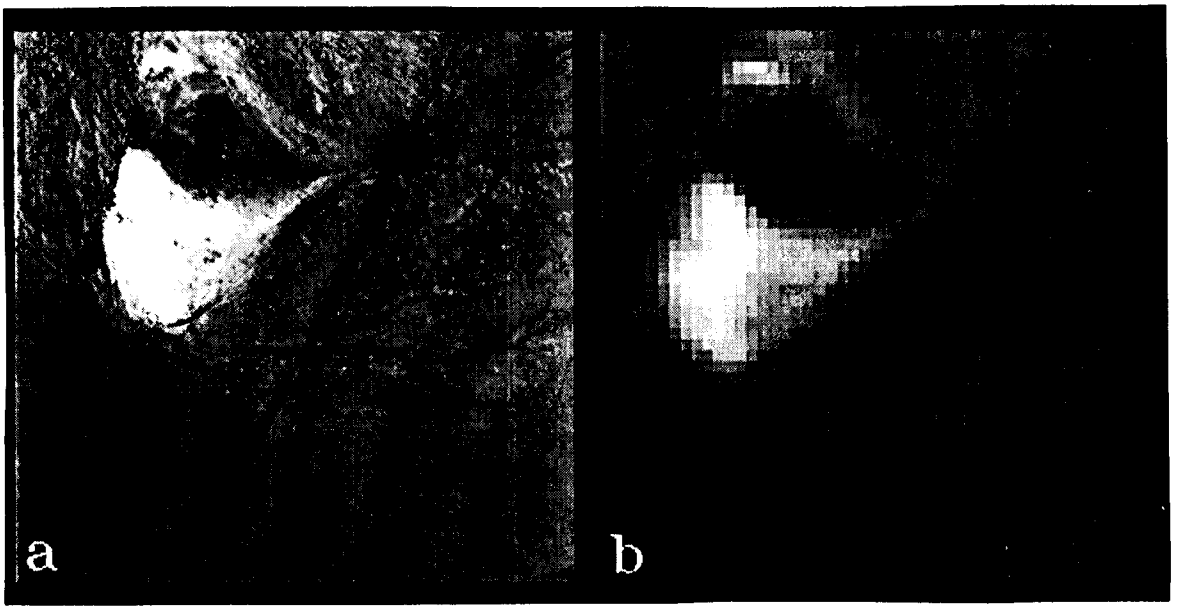

Figure 5. (a) HYDICE and (b) AVIRIS pair of abundance images of the kaolinite end member.

The central part of Kaolinite Hill is hematite-stained, altered tuff containing kaolinite. The 0.9 μm Fe^{3+} absorption is visible in the spectrum shown in figure 4. The abundance images of iron-stained kaolinite are shown in figure 6. The bright stripes at the edges of the HYDICE image are artifacts of the sensor dark current characteristics that are more pronounced beyond 2 μm. In general there is good correlation between the two abundance images.

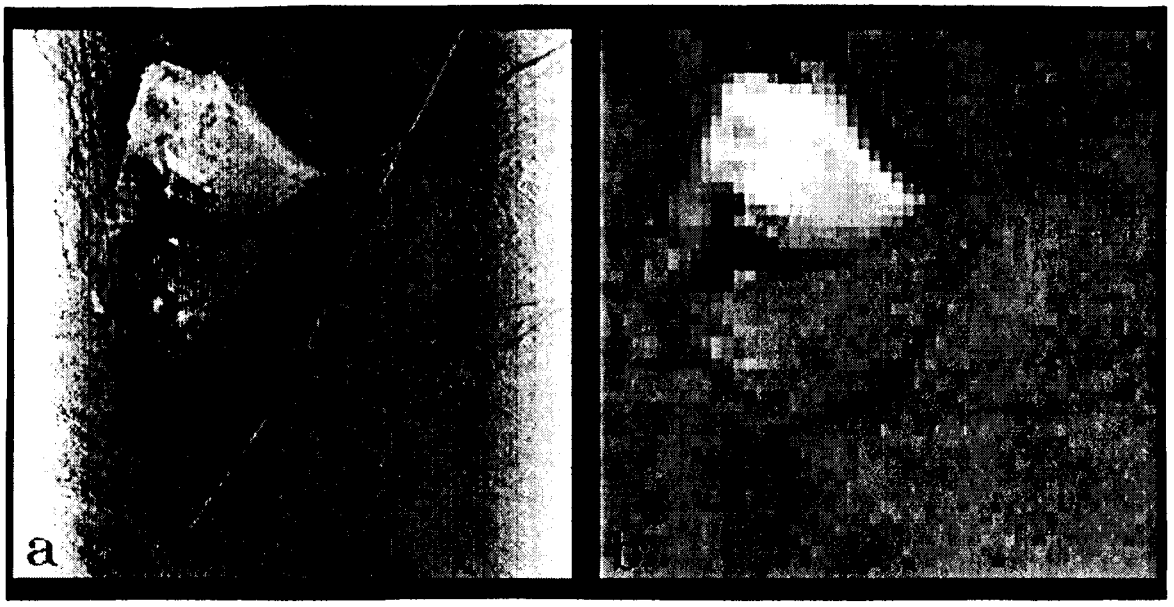

Figure 6. (a) HYDICE and (b) AVIRIS abundance images of the iron stained kaolinite end member.

Figure 7 shows the abundance of road material. The spectrum of the road end member is nearly identical to that of Kaolinite Hill short of 2.0 μm. In the HYDICE image these two end members are clearly differentiated while in the AVIRIS image Kaolinite Hill appears very dark, indicating a negative kaolinite component. The relatively evenly-spaced dark spots in the HYDICE image are clumps of sage brush.

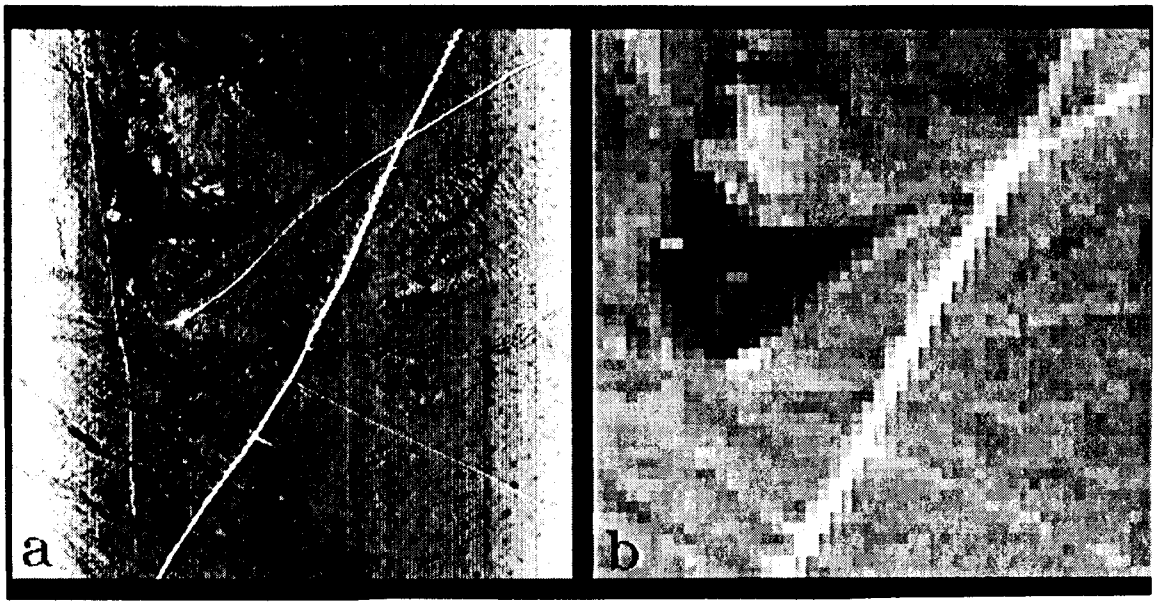

Figure 7. Abundance images for the road end member.

The power of unmixing analysis is shown in the AVIRIS image in which a jeep track running northwest from the lower right-hand corner of the image is seen. This track is approximately 2 m wide and less than 75% of road material is exposed. This represents approximately 1% of an AVIRIS pixel, a very small number. Of course, the road is only detectable because of its linear character.

The abundance images for the desert pavement end member are shown in figure 8. This figure demonstrates perhaps the best correlation between the two sensors. A clue to this agreement can be found in figure 3 that shows the nearly identical reflectance for desert pavement areas derived from HYDICE and AVIRIS short of 2.2 μm. The dark spots are sage brush clumps that are also faintly visible on the AVIRIS image. These clumps comprise less than 3% of an AVIRIS pixel.

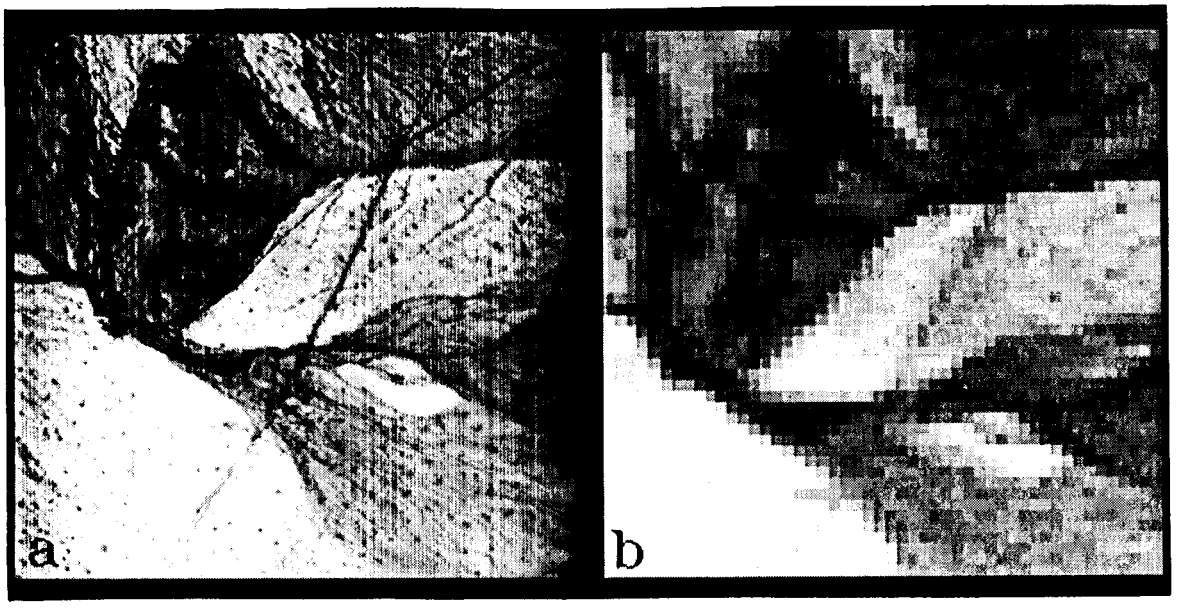

Figure 8. Abundance images of the desert pavement end member.

6. CONCLUSIONS

For the first time it has been possible to compare hyperspectral images from two sensors having a significantly different GIFOV. This factor of 36 difference in pixel area between HYDICE and AVIRIS has made it possible to choose appropriate and accurate end member spectra from the higher resolution sensor and use them in an unmixing analysis of both sensors.

The results show a high correlation between the abundance images of both sensors and indicate the accuracy and lack of major artifacts in the unmixing results derived from the lower resolution AVIRIS data.

7. ACKNOWLEDGMENTS

The authors wish to thank Kathy Heidebrecht of CSES for discussions and suggestions. This research was supported by contract number 66BP0192221 with the Desert Research Institute.

8. REFERENCES

Adams, J. B., Smith, M. O. and Gillespie, A. R., 1993, "Imaging spectroscopy: Interpretation based on spectral mixture analysis," in *Remote Geochemical Analysis: Elemental and Mineralogical Composition*, Pieters, C. M. and Englert, P. A., eds., Cambridge University Press.

Boardman, J. W., 1993, "Automating spectral unmixing of AVIRIS data using convex geometry concepts," *Proceedings Fourth Annual JPL Airborne Geoscience Workshops*, vol. 1, pp. 11-14.

Basedow, R. W., Armer, D. C. and Anderson, M. E., 1995, "HYDICE system: Implementation and performance, " *Proceedings SPIE*, vol. 2480, pp. 258-267.

Research Systems Inc., 1995 ENVI users manual.